The Strain Rate Dependency of Fracture in Polyethylene: Fracture Initiation

D. B. BARRY* and O. DELATYCKI, *Department of Industrial Science, University of Melbourne, Parkville, Victoria 3052, Australia.*

Synopsis

The dependency of fracture on the rate of strain of a range of polyethylene samples was measured in three point flexural tests at 23°C. The range of strain rates from 10^{-1} to 10^{-7} reciprocal seconds was examined. The J integrals at the initiation of the cracks were determined. This enabled the interrelationship between fracture initiation and the test rate to be established. The dependency follows a power law relation. The values of the exponents in the power law equations, derived from experiment, were found to be higher than the values calculated using established criteria for crack initiation. The difference is postulated to be due to the strengthening of the fibrils ahead of the crack because of the orientation of the fibrils in that region.

INTRODUCTION

High density polyethylene can fail under load in a brittle or ductile fashion. Generally, materials that are brittle are of limited engineering usefulness. As a rule, in applications such as plastics gas piping, ductile polyethylene grades are being used. The ductility of these materials imposes special conditions, if reliable measurements of their fracture resistance are to be obtained. The time dependency of polymeric materials introduces an added factor when determining their fracture behavior. These problems are investigated in the present work.

A number of fracture parameters have been suggested for the evaluation of the conditions for crack initiation in polyethylene. The J integral,[1,2] the stress intensity factor[3] K, and the crack opening displacement (COD) method[4,5] have all been used to study the fracture of HDPE. Both the J integral and the COD method were designed to study materials which exhibit significant deformation at the crack tip during the process of fracture.

The resistance of polyethylene to fracture is not fully defined by its resistance to crack initiation. Retarding the rate of propagation of the crack can result in a significant increase in the overall time to fracture a ductile material.

Investigations of the interrelation of the rate of crack propagation and strain rate have been reported previously.[6,7] Rates of crack initiation and propagation in polyethylene are determined by the morphology, molecular structure, and chemical composition of the material. Characterization of

*Present address: BHP Melbourne Research Laboratories, Mulgrave, Victoria 3170, Australia.

Journal of Applied Polymer Science, Vol. 38, 339–350 (1989)
 CCC 0021-8995/89/020339-12$04.00

TABLE I
Materials Tested

Material	M_n $\times 10^3$ (a.m.u.)	M_w/M_n	Density (g/cm^3)	Melting point (°C)	Crystallinity X_c (%)
1	10.4	12.4	0.970	135	75
2	9.5	12.0	0.960	132	69
3	19.6	5.2	0.943	130	63
4	15.3	9.2	0.962	131	60
5	19.2	6.1	0.951	134	66
6	10.1	10.2	0.961	136	75

specimens used in fracture studies is necessary for a better understanding of the process. This subject will be examined further in our next article.

Numerous grades and makes of HDPE have been tested. Those reported in this article are listed in Table I. All samples are commercial pipe grade resins. The materials were compression-molded in a temperature programmable press to produce blocks from which samples for the fracture studies were machined. The temperature cycle used in the press was:

(i) 180°C for 30 min,
(ii) cool at 1°C/min to 130°C,
(iii) hold at 130°C for 120 min,
(iv) cool 1°C/min to ambient temperature.

Microtomed sections showed the specimens to contain spherulites with radii of between 10 and 20 μm. Table I gives the molecular weight, density, and crystallinity of the samples. The molecular weights of the samples were determined on a Waters 150C gel permeation chromatograph at 140°C, using dichlorobenzene, with 1% of thermal stabilizer. Density was determined by weight difference when immersed in 1-propanol. Crystallinities were calculated, using X-ray spectra, as the ratios of the areas under the crystalline peaks to the total areas under the peaks.

MECHANICAL TESTING

The modulus E and the yield stress σ_Y, were determined from measurements at a range of strain rates from 10^{-1} to 10^{-6} s^{-1} and at a temperature of 23 $\pm$ 2°C. The relationship between the strain rate $\dot{e}$ and both E and σ_Y can be described by power law equations. The coefficients for these equations and the goodness of fit, R^2, of the data are given in Table II. In all cases the fit of the data was better than 85%.

FRACTURE TESTING

Specimens were tested in three point bending. A span to width ratio of 4 was used. The sample geometry and dimensions are shown in Figure 1. All specimens were tested at 23°C. Two testing procedures were used. Specimens of 3 mm breadth were tested using a continuous crack length observation

TABLE II
Power Law fit of E and σ_Y to $\dot{e}$

Material	$E = E_0\dot{e}^n$			$\sigma_Y = \sigma_0\dot{e}^m$		
	E_0	n	R^2	σ_0	m	R^2
1	268	0.0742	0.90	38	0.0746	0.99
2	202	0.0820	0.97	32	0.0696	0.99
3	147	0.0873	0.98	27	0.0641	0.99
4	259	0.1036	0.85	30	0.0625	0.99
5	321	0.1784	0.96	34	0.0682	0.97
6	315	0.0529	0.87	36	0.0621	0.93

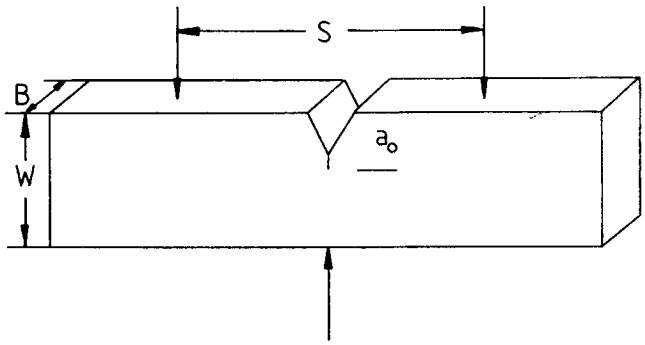

Fig. 1. The fracture test geometry and specimen dimensions.

technique. All other specimens had breadths of 15 mm or greater. For these specimens a multispecimen technique was used, as the crack tips cannot be observed, because they are obscured by plane stress stretch zones at the boundaries of the cracks.

The widths, W of the specimens were either 30 or 40 mm; the breadths B were 3, 15, 25, and 54 mm. The initial crack depth to width ratios, a_0/W, of specimens with the breadth of 3 mm (B = 3 mm), were varied between 0.2 and 0.7. In all other specimens the initial crack depth to width ratio was invariant at 0.5. A notch was machined into the specimens. This blunt machined notch was extended using a razor impressing technique. This method of crack sharpening has been used widely.[8,9]

FRACTURE ANALYSIS

Pipe grade HDPE is a tough polymer at 23°C. The analysis of fracture in these types of materials requires a parameter that takes into account crack tip plasticity. One such parameter is the J integral. The J integral may be defined as the partial derivative of energy with respect to crack length, at a constant deflection:

$$J = \frac{1}{B}\frac{\delta U}{\delta a}\Bigg]_{\delta} \tag{1}$$

Equation (1) was used to analyze the fracture of the B = 3 mm specimens.

This analysis follows the work by Hodgkinson and Williams.[10] A simpler form of eq. (1) is given in

$$J = 2U/B(W - a_0) \tag{2}$$

Equation (2) is and approximation of eq. (1), and can be used successfully if the samples are deeply notched and tested in bending. Equation (2) was used in conjunction with the multispecimen testing technique of Begley and Landes[11] that was employed to determine the fracture resistance of specimens of breadths greater than 15 mm. The experimental procedures used for testing both thin (B = 3 mm) and thick ($B \geq 15$ mm) specimens will be discussed in a later section of this paper.

The J integral is an energy-based fracture parameter. Stress intensity values K were calculated using

$$K = (JE)^{1/2} \tag{3}$$

Crack initiation occurs at a critical value of J or K. A critical value of the J integral, J_c can be determined by plotting the J integral as a function of the change in crack length, Δa, and extrapolating the data to $\Delta a = 0$. If, during

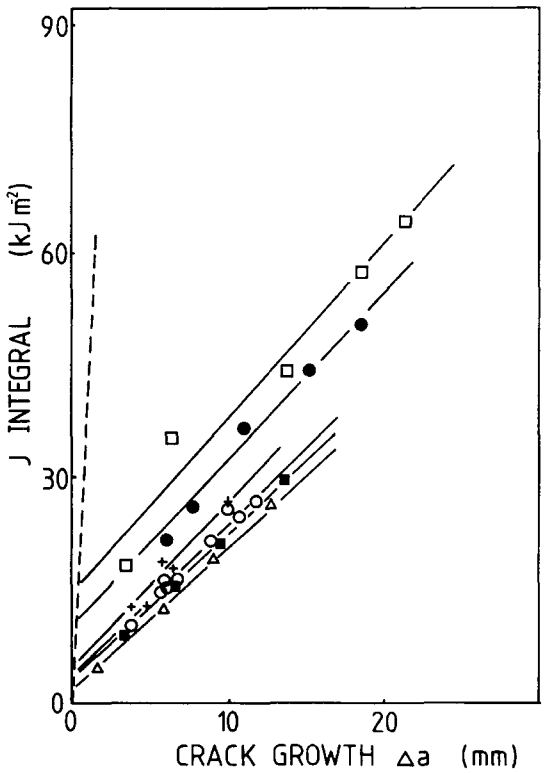

Fig. 2. $J(\Delta a)$ curves for material 1 at a range of strain rates: (□) 0.1 s^{-1}; (●) 0.02 s^{-1}; (+) 0.002 s^{-1}; (○) 2 × 10^{-4} s^{-1}; (■) 2 × 10^{-6} s^{-1}; (△) 2 × 10^{-7} s^{-1}. The crack blunting line is shown as dashed.

cracking, crack blunting occurs, extrapolation of the $J(\Delta a)$ data back to zero underestimates the value of J_c. This is because crack blunting acts as a pseudoextension of the crack. To account for crack blunting, a crack blunting line is used. Equation (4) is one of the equations that is used to account for crack blunting[1]:

$$J = 2\,\Delta a \sigma_Y \tag{4}$$

The blunting line for each strain rate was calculated using the coefficients given in Table II. All values of J_c were read at the intersection of the line described by eq. (4) and the $J(\Delta a)$ line.

The dependence of J_c on the breadth of the specimen was investigated. Specimen dimensions that give size independent values of J_c are necessary to allow valid comparisons of fracture resistances for a range of materials and strain rates. The results for B = 3 mm specimens were included to determine an upper value of fracture resistance.

EVALUATION OF J INTEGRAL, B = 3 mm

Testing of samples 3 mm broad was performed according to the method of Hodgkinson and Williams.[10] In these tests the length of the growing crack was measured using a traveling microscope. As the crack passed a set of predeter-

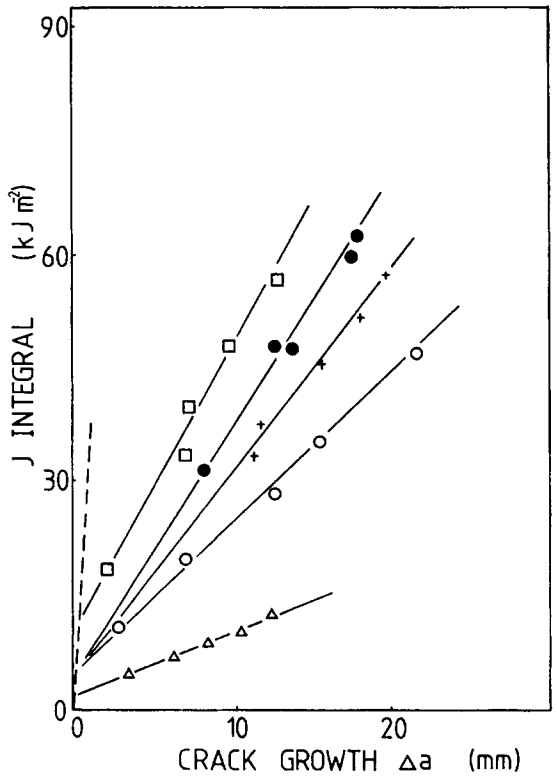

Fig. 3. $J(\Delta a)$ curves for material 2 at a range of strain rates: (□) 0.1 s^{-1}; (●) 0.02 s^{-1}; (+) 0.002 s^{-1}; (○) 2 × 10^{-4} s^{-1}; (△) 2 × 10^{-7} s^{-1}. The crack blunting line is shown as dashed.

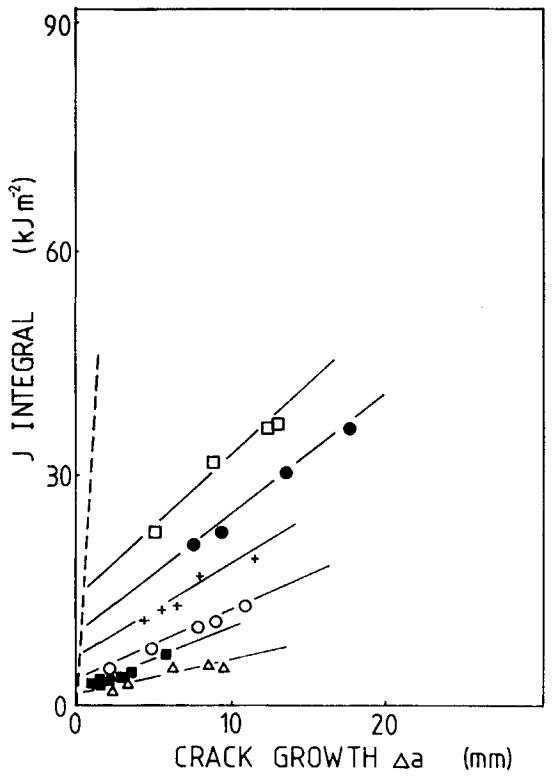

Fig. 4. $J(\Delta a)$ curves for material 3 at a range of strain rates: (□) 0.1 s^{-1}; (●) 0.02 s^{-1}; (+) 0.002 s^{-1}; (○) 2×10^{-4} s^{-1}; (■) 2×10^{-6} s^{-1}; (△) 2×10^{-7} s^{-1}. The crack blunting line is shown as dashed.

mined crack lengths, the load–deflection diagram was marked. The load–deflection–crack length diagrams, each for a different initial crack length, were used to determine the $J(\Delta a)$ line for the material. The intersection of this line with the blunting line [eq. (4)] gave the critical value of J at crack initiation.

EVALUATION OF THE J INTEGRAL; $B \geq 15$ mm

The multispecimen technique of Begley and Landes[11] was used to determine the $J(\Delta a)$ data for the thick specimens. This method consists of loading a series of identical specimens to a range of deflections. This produces cracks of different lengths, Δa, in the specimens. The specimens were unloaded and broken after immersion in liquid nitrogen. Thus the crack growth in each specimen was measured. The J integrals for these fractures were calculated using eq. (2). The energy under the load–deflection curve (U) was determined using a planimeter. The $J(\Delta a)$ values were plotted to give a crack growth resistance curve. The critical value of the J integral, J_c at the initiation of the crack is the value of the intersection of the $J(\Delta a)$ regression line and the $2\,\Delta a \sigma_Y$ blunting line. At least five specimens were tested at each strain rate. The $J(\Delta a)$ curves for each material that was tested are given in Figures 2–7.

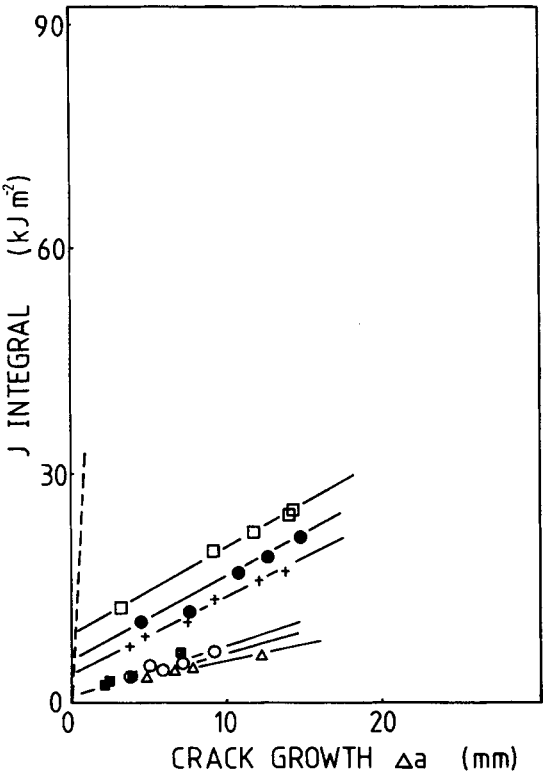

Fig. 5. $J(\Delta a)$ curves for material 4 at a range of strain rates: (□) 0.1 s^{-1}; (●) 0.02 s^{-1}; (+) 0.002 s^{-1}; (○) 2×10^{-4} s^{-1}; (■) 2×10^{-6} s^{-1}; (△) 2×10^{-7} s^{-1}. The crack blunting line is shown as dashed.

The crack blunting line at a strain rate of 2×10^{-4} s^{-1} (1 mm/min), was included in the figures to illustrate the method of determination of J_c.

THE EFFECT OF SPECIMEN DIMENSIONS

To establish a valid correlation between strain rate and J integral, the value of the J integral must be independent of specimen size and testing geometry. To establish the dependency of J_c on specimen breadth, J_c was determined as a function of B at 0.02, 0.002, and 2×10^{-4} s^{-1}. A typical set of data for J_c vs. B at 0.002 s^{-1} is given in Figure 8, ASTM E399 provides a criterion for the minimum specimen size. The energy equivalent of the size criterion is given in:

$$a, B, (W - a_0) \geq 25 J_c/\sigma_Y \tag{5}$$

The values for the minimum size requirements, obtained from eq. (5) for the materials test, are marked on the curves in Figure 8. Equation (5) seriously underestimates the minimum size required for material 2. Figure 8 also shows that at a strain rate of 0.002 s^{-1} a minimum specimen dimension of between 10 and 15 mm is adequate for size independent estimates of J_c for all materials but 2. For material 2 this minimum dimension is at least 40 mm.

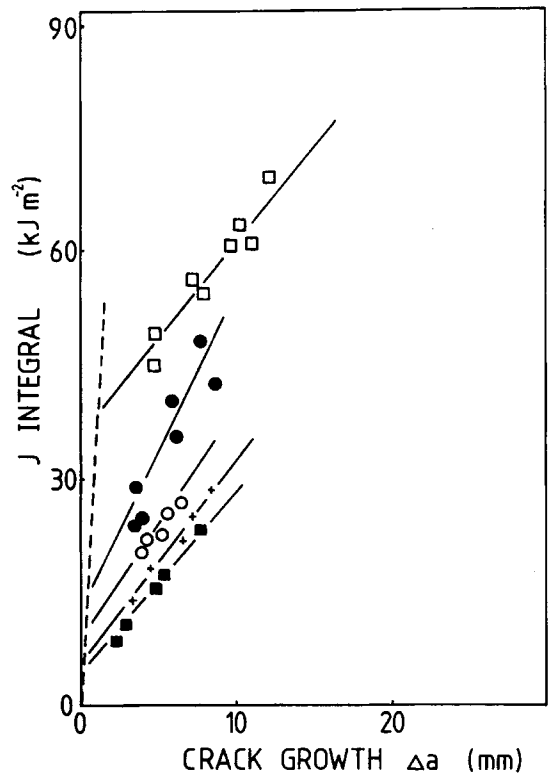

Fig. 6. $J(\Delta a)$ curves for material 5 at a range of strain rates: (□) 0.1 s^{-1}; (●) 0.02 s^{-1}; (+) 0.002 s^{-1}; (○) 2×10^{-4} s^{-1}; (■) 2×10^{-6} s^{-1}. The crack blunting line is shown as dashed.

The size independent values of J_c are given in Table III. Table III also contains the values of K_c. These values were calculated using eq. (3).

FRACTURE RESISTANCE–STRAIN RATE

Williams[12] has suggested that the stress intensity factor K_c, is related to the strain rate $\dot{e}$. The exact relationship depends on the choice of the crack initiation criterion. Two criteria for crack initiation have been suggested. The first assumes that crack initiation occurs when the fibrils at the root of the crack reach a critical extension. Crack opening displacement (COD) is a measure of the extension of the fibrils at the tip of the crack. If COD controls crack initiation, Williams has shown that the dependency between K_c and $\dot{e}$ takes the form of

$$K_c \propto \dot{e}^{(m+n)/2} \tag{6}$$

The second criterion for crack initiation rests on the assumption that initiation occurs once a critical energy barrier has been overcome. For this criterion the relationship between K_c and $\dot{e}$ is given by

$$K_c \propto \dot{e}^{n/2} \tag{7}$$

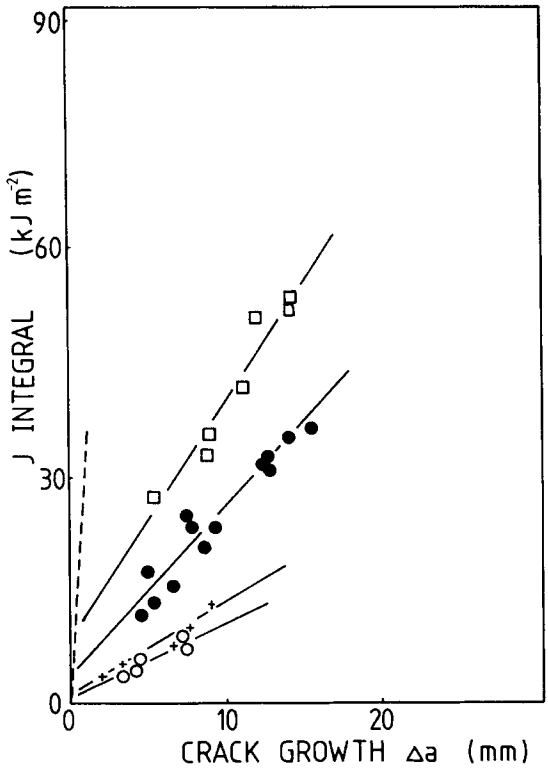

Fig. 7. $J(\Delta a)$ curves for material 6 at a range of strain rates: (□) 0.1 s^{-1}; (●) 0.02 s^{-1}; (+) 0.002 s^{-1}; (○) 2×10^{-4} s^{-1}. The crack blunting line is shown as dashed.

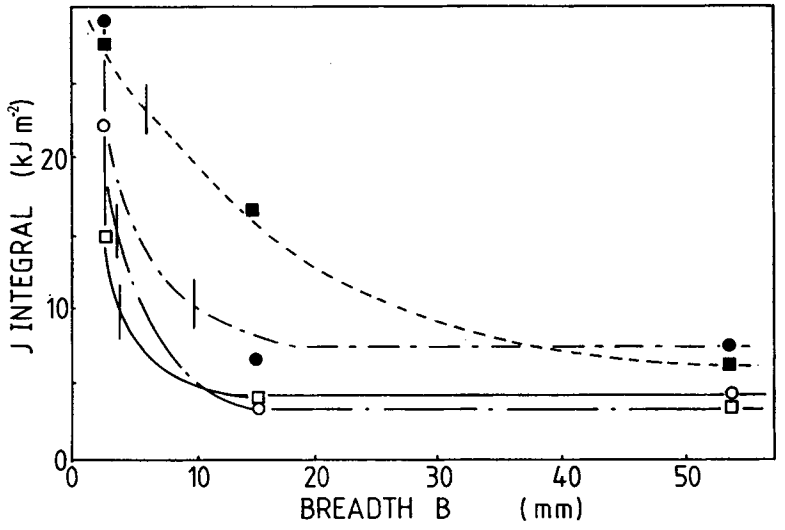

Fig. 8. J_c vs. B data for materials 1 (○), 2 (■), 3 (●), and 4 (□) at a strain rate of 0.002 s^{-1}.

TABLE III
J_c and K_c Values for the Materials[a]

Material	1		2		3		4		5		6	
strain rate $\dot{e}$ (s^{-1})	J_c	K_c	J_c	K_c	J_c	K_c	J_c	K_c	J_c	K_c	J_c	K_c
0.1	15.4	1.9	13.6	1.5	15.3	1.4	9.6	1.4	40.0	2.9	8.4	1.6
0.02	6.8	1.2	16.4	1.5	10.0	1.0	6.4	1.0	7.3	1.1	4.3	1.0
0.002	3.6	0.8	6.0	0.7	7.0	0.8	3.8	0.7	6.4	0.8	0.9	0.5
2×10^{-4}	3.1	0.7	10.6	1.0	2.3	0.5	1.3	0.4	1.6	0.4	1.9	0.6
2×10^{-6}	3.0	0.7	2.1	0.3	2.5	0.4	2.1	0.3				
2×10^{-7}	2.0	0.4	2.0	0.4	1.7	0.3	2.9	0.4				

[a] J_c has units of kJ m^{-2}; K_c has units of MPa $m^{1/2}$.

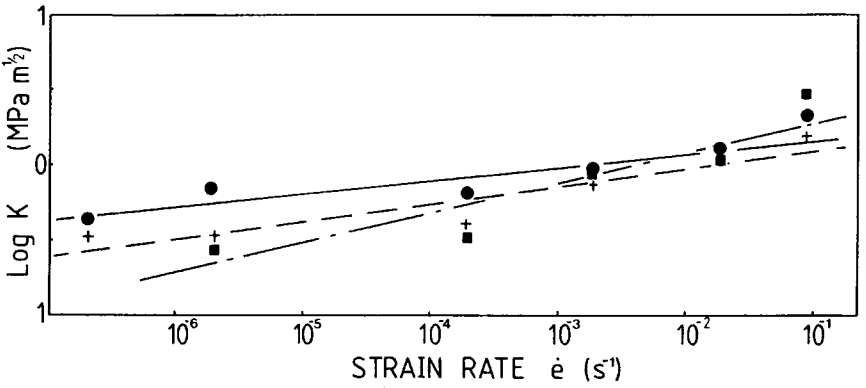

Fig. 9. K_c vs. log $\dot{e}$ for materials 1 (●), 3 (+), and 5 (■).

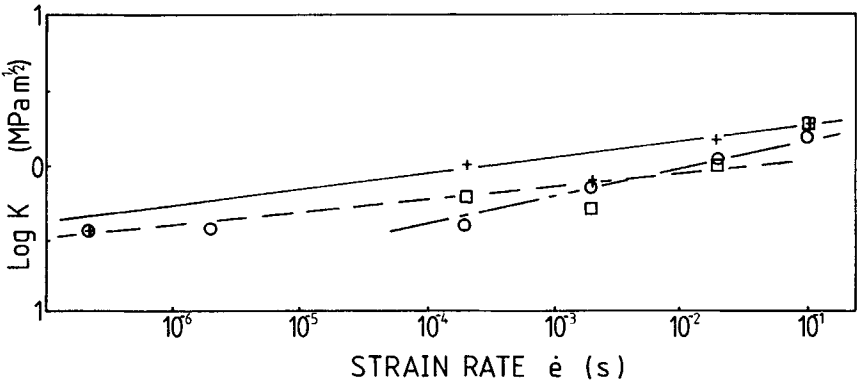

Fig. 10. K_c vs. log $\dot{e}$ for the materials 2 (+), 4 (○), and 6 (□).

The $K_c(\dot{e})$ data for the materials tested are plotted in Figures 9 and 10. Least squares lines have been fitted to the data and they are shown in the figures. The coefficients of the regression analyses are given in Table IV. This table also contains the values of the coefficient of determination, R^2, which shows that these lines describe the data well. The predicted exponents, as calculated from eq. (6) and (7), are also given in Table IV. Comparison of the exponents

TABLE IV
Comparison of Crack Initiation Components; Fitted equation $K_c = a\dot{\epsilon}^b$

Material	a	b	R^2	$(m + n)/2$ [eq. (6)]	$n/2$ [eq. (7)]
1	1.86	0.106	0.90	0.074	0.037
2	2.24	0.105	0.89	0.041	0.082
3	1.71	0.136	0.95	0.076	0.044
4	1.46	0.104	0.78	0.083	0.052
5	3.19	0.215	0.87	0.123	0.089
6	1.95	0.165	0.71	0.058	0.026

obtained by experiment (column 3) and those calculated assuming the COD criterion (column 5) and the energy criterion (column 6) indicate that the COD criterion better describes the experimental results.

DISCUSSION

The values of the strain rate exponents, calculated using the experimental results, are larger than those obtained from eq. (6) and (7). This indicates that the materials tested have a greater resistance to crack initiation than predicted using the theories. The exponents obtained experimentally show that fracture resistance of the materials is more sensitive to changes in strain rate than predicted by eq. (6) and (7). There are two possible reasons for the enhanced fracture resistance and strain rate sensitivity of the materials.

The fibrilar region at the tip of the crack is highly anisotropic. The material properties of this region are significantly different from those of the bulk material. In general, the properties of polyethylene can be enhanced by drawing and orientation. The fibrilar region contains ties in which considerable molecular orientation has occurred. These ties form strong connections between the adjacent weaker elements of the bulk material. As the tip of the crack opens, these strong fibrils draw more material from the adjacent bulk polymer. This extending and aligning results in enhanced fracture resistance. The COD criterion takes no account of fibril orientation and the associated improvement in the modulus and strength of the fibrils.

Another explanation for the rate dependence and increased fracture resistance is that thermal softening occurs within the fibrils. This temperature increase is caused by dissipation of the energy associated with the deformation of the fibrils. This could explain the difference between the predicted and experimental values of fracture toughness at higher strain rates. The higher the strain rate, the greater the deformation rate within the fibrils, resulting in increased thermal softening. It seems unlikely that thermal softening is important at the slower strain rates.

The results shows that fracture resistance is strain-rate-dependent. This is not unexpected as other properties of polymers are strain-rate-dependent. The nature of this dependency gives some insight into the molecular nature of the fracture mechanism.

CONCLUSIONS

The J integral has been applied successfully to determine the initiation of fracture in a range of polyethylene samples over a range of strain rates. The stress intensity factor K, derived from the J integral, has been found to be related to the strain rate $\dot{e}$ by a power law relationship. The predicted value of the exponents in the power law relationship, using the COD criterion, were found to be significantly lower than values obtained from experiments. This difference is postulated to be due to the increased stiffness of the fibrils in the crack zone, caused by molecular orientation within the fibrils. The minimum size of the specimen to obtain size-independent results was also evaluated. In one case the ASTM minimum size criterion appears to be low.

APPENDIX: NOMENCLATURE

a_0 initial crack length (mm)
Δa change in crack length (mm)
B specimen breadth (mm)
$\dot{e}$ strain rate (s^{-1})
E Young's Modulus (MPa)
J J integral (kJ m^{-2})
K stress intensity Factor (MPa $m^{1/2}$)
R^2 coefficient of goodness of fit
S span (mm)
U energy (J)
W specimen width (mm)
δ deflection (mm)
σ_Y yield strength (MPa)

References

1. M. K. V. Chan and J. G. Williams, *Int. J. Fract.*, **23**, 145 (1983).
2. I. Narisswa, *Polym. Eng. Sci.*, **27**, 41 (1987).
3. M. K. V. Chan and J. G. Williams, *Polym. Eng. Sci.* **21**, 1019 (1981).
4. X. Lu and N. Brown, *J. Mater. Sci.*, **21**, 4081 (1986).
5. X. Lu and N. Brown, *J. Mater. Sci.*, **21**, 423 (1986).
6. J. G. Williams and G. P. Marshall, *Proc. R. Soc. Lond.*, **A342**, 55 (1975).
7. G. P. Marshall, *Plastics and Rubber: Processing and Applications*, **2**, 169 (1982).
8. M. K. V. Chan and J. G. Williams, *Polymer*, **24**, 234 (1983).
9. N. Brown and S. K. Bhattacharya, *J. Mater. Sci.*, **20**, 4552 (1985).
10. J. M. Hodgkinson and J. G. Williams, *J. Mater. Sci.*, **16**, 50 (1981).
11. J. A. Begley and J. D. Landes, *American Society for Testing and Materials Special Tech. Publ.*, ASTM, Philadelphia, 1972, Vol. 514, p. 1.
12. J. G. Williams, in *Fracture Mechanics of Polymers*, Ellis Horwood, New York, 1984, p. 176.

Received April 18, 1988
Accepted July 18, 1988